

**Supplementary Information to
“Unraveling the role of Sm 4f electrons in the magnetism of SmFeO₃”**

Danila Amoroso,¹ Bertrand Dupé,^{2,1} and Matthieu J. Verstraete³

¹*Nanomat/Q-mat/CESAM, Université de Liège, B-4000 Sart Tilman, Belgium*

²*Fonds de la Recherche Scientifique (FNRS-FRS), B-1000 Brussels, Belgium*

³*Nanomat/Q-mat/CESAM, Université de Liège, and European Theoretical Spectroscopy Facility, B-4000 Sart Tilman, Belgium*

Atomic pairs	Pbnm w/ Sm-f (Å)	Exp.[1] (Å)	Pbnm w/o Sm-f (Å)	RE w/ Sm-f	RE w/o Sm-f
Sm ₁ -Sm _{2(2')}	3.7975	3.7909	3.7604	0.17%	-0.81%
Sm ₁ -Sm ₃ ($\times 2$)	3.9011	3.9087	3.9139	-0.20%	0.13%
Sm _{1'} -Sm _{2(2')}	3.9882	3.9910	4.0091	-0.07%	-0.17%
Fe ₁ -Fe ₃ ($\times 2$)	3.8498	3.8530	3.8451	-0.08%	-0.21%
Fe ₁ -Fe ₂ ($\times 4$)	3.8916	3.8896	3.8826	0.05%	-0.18%
Fe _{1(1'')} -Sm ₁₍₃₎	3.1486	3.1406	3.1199	0.25%	-0.66%
Fe _{1(1')} -Sm ₂₍₄₎	3.2782	3.2740	3.2446	0.13%	-0.90%
Fe _{1'(1)} -Sm ₂₍₄₎	3.3895	3.3908	3.3902	-0.04%	-0.02%
Fe _{1''(1)} -Sm ₁₍₃₎	3.6549	3.6682	3.7030	-0.36%	0.95%
Fe ₃ -O ₁₍₂₎	2.0303	2.0276	2.0320	0.14%	0.21%
Fe ₃ -O ₃₍₄₎	2.0100	2.0008	2.0079	0.46%	0.36%
Fe ₃ -O ₉₍₁₀₎	1.9984	2.0120	2.0025	-0.68%	-0.47%
Sm ₂ -O ₃₍₈₎	2.3356	2.3370	2.3378	-0.06%	-0.18%
Sm ₂ -O ₄₍₇₎	2.7014	2.7026	2.7085	-0.04%	0.22%
Sm ₂ -O _{9'}	2.3084	2.3090	2.2987	-0.03%	-0.45%
Sm ₂ -O _{12'}	2.4017	2.3880	2.3653	0.57%	-0.95%
Sm ₂ -O ₂₍₅₎	2.5840	2.5730	2.5291	0.43%	-1.71%
Sm ₂ -O ₁₍₆₎	3.4804	3.4930	3.5273	-0.36%	0.98%
Sm ₂ -O ₉	3.1827	3.1800	3.1663	0.09%	-0.43%
Sm ₂ -O ₁₂	3.3178	3.3370	3.3948	-0.57%	1.73%
Sm _{1(1')} -Sm ₄ ($\times 2$)	5.1865	—	5.1364	—	—
Sm ₁ -Sm _{1'} ($\times 2$)	5.4086	5.3995	5.3594	0.17%	-0.74%
Sm ₂ -Sm _{2'} ($\times 2$)	5.5969	5.6001	5.6191	-0.06%	0.34%
Sm _{1(1')} -Sm _{4'} ($\times 2$)	5.8127	—	5.8599	—	—
Fe ₁ -Fe _{1'} ($\times 2$)	5.4086	5.3995	5.3594	0.17%	-0.74%
Fe ₁ -Fe ₄ ($\times 8$)	5.4740	—	5.4643	—	—
Fe ₁ -Fe _{1''} ($\times 2$)	5.5969	5.6001	5.6191	-0.06%	0.34%
Fe _{1'} -Fe _{1'}	7.6995	7.7060	7.6902	-0.08%	-0.21%
Interatomic angles					
\angle Fe ₁ -O ₆ -Fe ₂	148.81°	148.64°	147.51°	0.12%	-0.76%
\angle Fe ₁ -O ₉ -Fe ₃	148.83°	148.67°	147.91°	0.10%	-0.51%
\angle O ₁₀ -Fe ₃ -O ₂	88.72°	88.74°	88.73°	-0.03%	-0.01%
\angle O ₁₀ -Fe ₃ -O ₄	88.86°	88.75°	88.46°	0.13%	-0.32%
\angle O ₁₀ -Fe ₃ -O ₉	180.00°	180.00°	180.00°		

Table SI. Interatomic distances and angles properties calculated for the orthorhombic Pbnm SmFeO₃ either excluding (w/o) or including (w/) Sm-f electrons as valence states. Room temperature experimental data from Ref. [1] and relative errors (RE) are also reported. Atomic labels refer to labeling in Fig. 1(b) in the main-text.

[1] E. N. Maslen, V. A. Streltsov, and N. Ishizawa, Acta Crystallographica Section B **52**, 406 (1996).

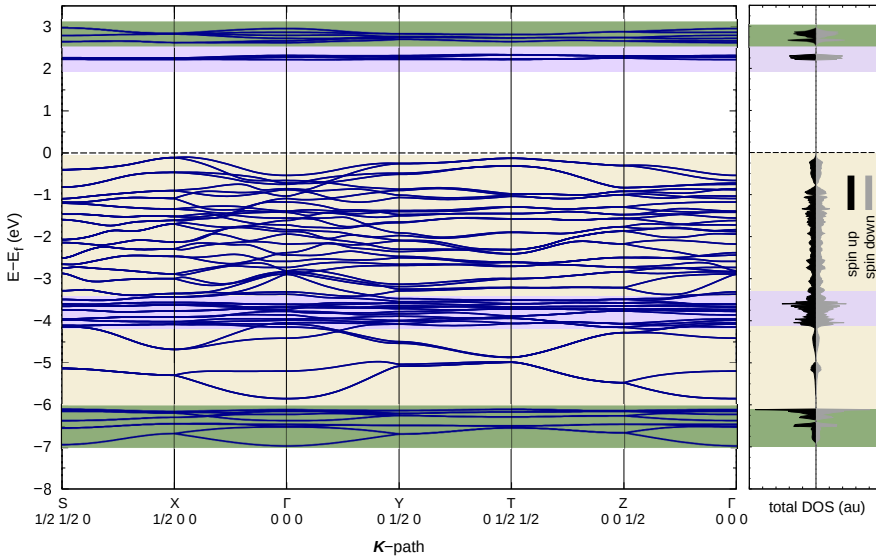


Figure S1. Electronic bands structure of collinear antiferromagnetic SmFeO₃, with **G**-type spin order for both Sm and Fe sub-structures. Total density of states (DOS) for spin-up and spin-down channel is also shown. Colored area identify different atomic bands character: green mainly Fe-*d* contribution, violet mainly Sm-*f* contribution, yellow mainly O-Fe contribution. Orbital-resolved DOS are shown in Fig. 2 of the main-text.

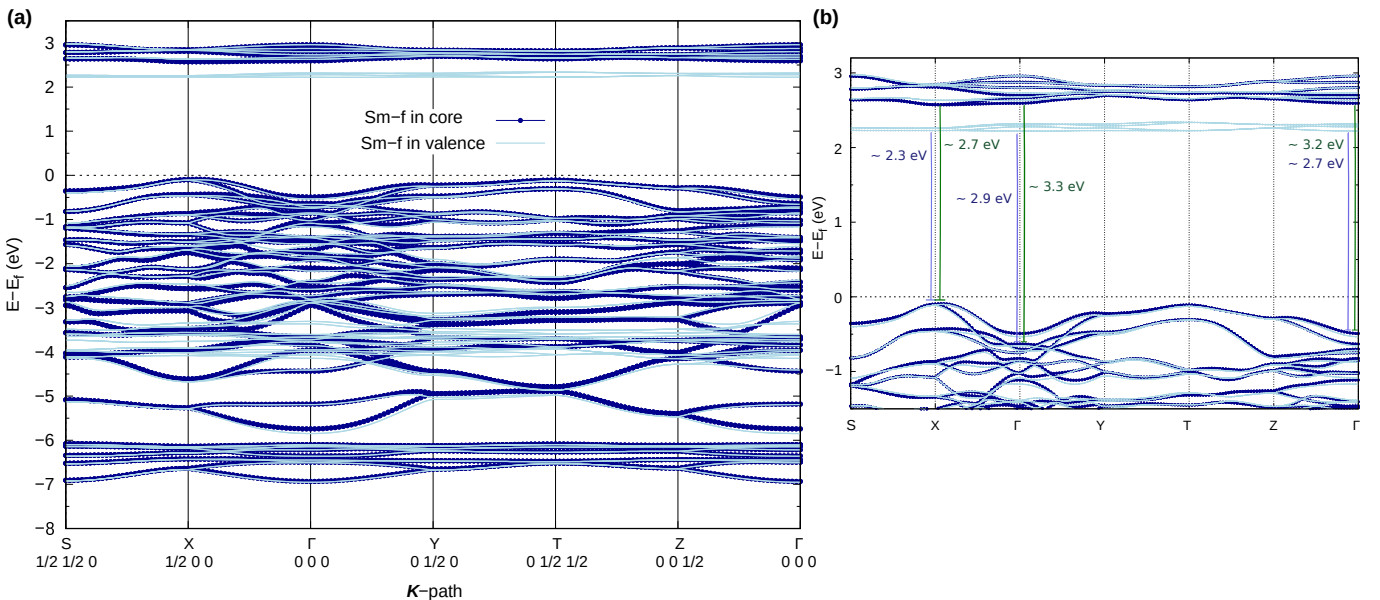


Figure S2. (a) Comparison of electronic bands obtained from including (light-blue line) and excluding (dark-blue line) Sm-*f* electrons in the valence states; same Hubbard-*U* value is added on Fe for the two cases, i.e. 4.5 eV. Underlying atomic structure has been relaxed within the two conditions. It is clear the Sm-*f* states do not affect the overall electronic properties, but add the relative states. (b) Zoom highlighting different energy gap at Γ and out-of- Γ , also considering the bottom either of the Sm-*f* (violet line) or Fe-*d* (green line) conduction bands.

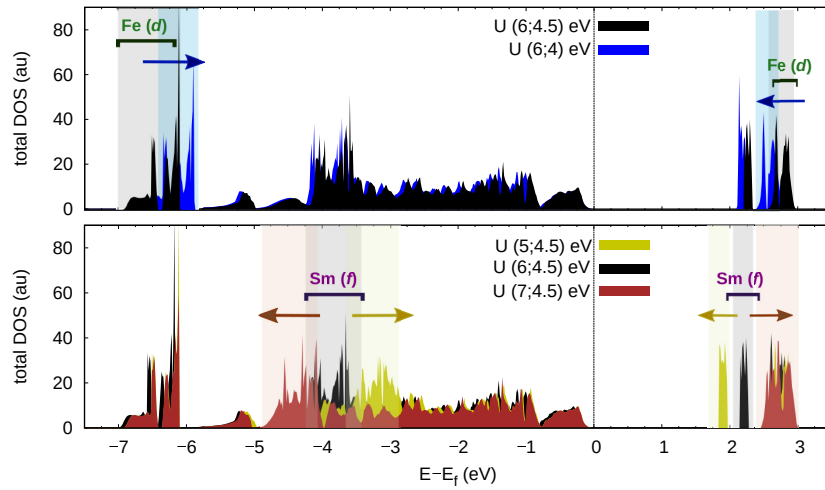


Figure S3. Effect of different Hubbard- U values on the electronic properties of antiferromagnetic SmFeO_3 , with G-type spin order for both Sm and Fe sub-structures. Only DOS from spin-up channel is shown. (top) Total DOS changing U -correction on Fe- d states from 4.5 eV to 4 eV. (bottom) Total DOS changing U -correction on Sm- f states from 6 eV to 5 eV and 7 eV. Energy shifts of the d - and f -states are highlighted. Underlying crystal structure is fixed to the one obtained relaxing with $U(6;4.5)$ eV on Sm and Fe.

A variation of U from 4.5 eV to 4 eV on Fe- d states translates (by about 0.25 eV) the Fe- d state peaks up at the VB top and the Sm- f and Fe- d states peaks down at the CB bottom; no substantial changes in the hybridization or spin-polarization are observed. A variation of U from 6 eV to 5 eV on Sm- f states produces upward and downward shifts of the Sm- f states in the VB and CB, respectively; *vice versa*, for $U=7$ eV, with an overlap of the Fe- d and Sm- f higher energy states (CB).

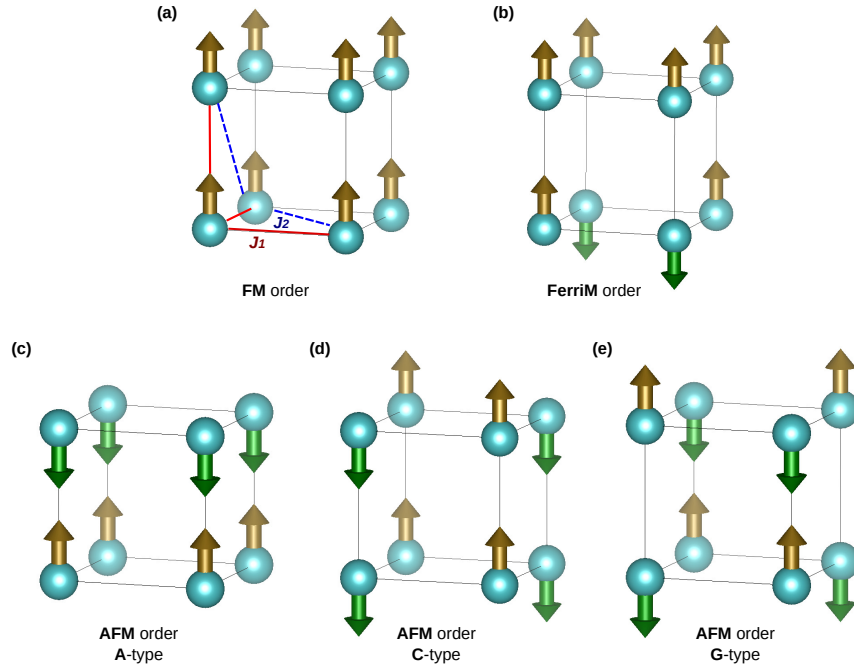


Figure S4. Schematic view of (a) ferromagnetic (FM), (b) ferrimagnetic (FerriM) and antiferromagnetic (AFM) (c) A-type, (d) C-type, (e) G-type collinear spin orders for the pseudo-cubic Sm- and Fe- atomic substructures in orthorhombic SmFeO_3 . Sketch of first- (J_1) and second- (J_2) neighbour interactions is also shown in (a).

spin configuration		U(6;4.5) eV	U(5;4.5) eV	U(7;4.5) eV	U(6;4) eV	w/o Sm-f U(0;4.5) eV	
Sm-order	Fe-order	ΔE (meV/f.u.)	ΔE (meV/f.u.)	ΔE (meV/f.u.)	ΔE (meV/f.u.)	Fe-order	ΔE (meV/f.u.)
FerriM	G	0.00	0.00	0.00	0.00	G	0.00
	C	-0.40	-0.49	-0.35	-0.40		
	FM	-0.19	—	—	-0.18		
	G	-0.02	-0.23	+0.10	-0.01		
	C	+60.58	+59.65	+61.24	+64.41	C	+61.59
	FM	+63.59	+63.20	+63.47	+67.29		
G	FerriM	+103.26	—	—	+110.16	FerriM	+102.55
FM	FerriM	+105.04	—	—	+111.87		
A	A	+136.05	+135.62	+136.34	+145.03	A	+137.00
FM	A	+136.40	+135.87	+136.73	+145.38		
FM	FM	+219.86	+220.06	+219.43	+234.85	FM	+214.72

Table SII. Energy differences between various collinear spin orders as a function of different Hubbard- U corrections [$U(\text{Sm};\text{Fe})$ eV]. Underlying crystal structure is fixed to the one obtained relaxing within **G-G** spin order for the Sm- and Fe- spin substructures and U -correction of (6;4.5) eV on Sm- f and Fe- d electronic states, respectively. At variance, the energy differences in the last column have been calculated by freezing the Sm-4f electrons in the core and we used the related optimized **G**-type structure. Schematic visualization of the different magnetic sub-substructures is shown in Fig. S4.

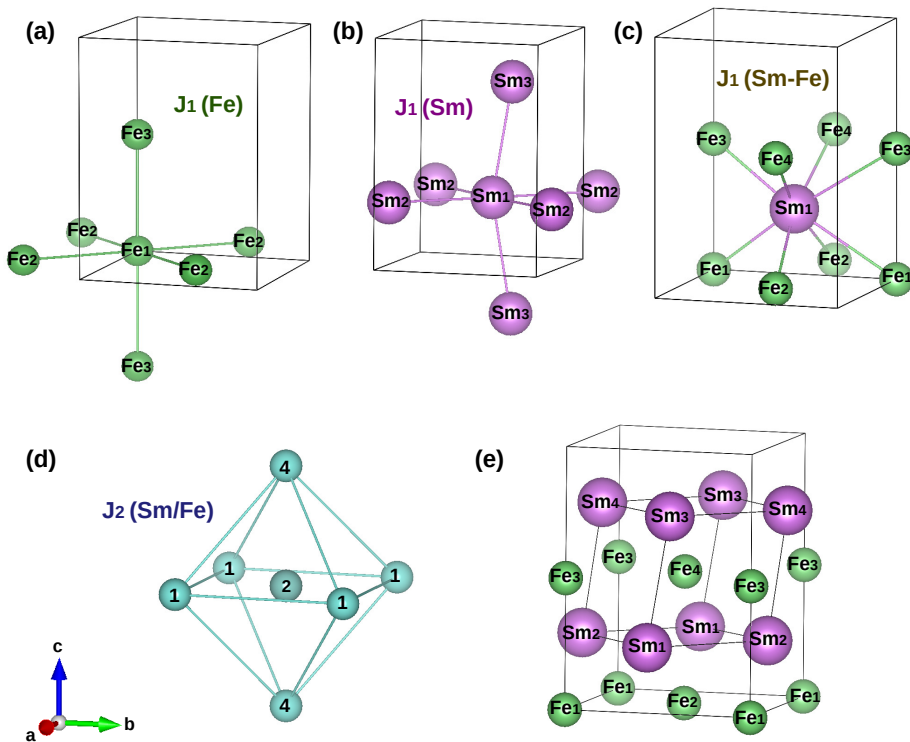


Figure S5. Examples of coordination for the considered nearest neighbour atomic pairs, defining effective, average first- (J_1) and second- (J_2) neighbour magnetic interactions; as an approximation, all atoms of the same species are treated as structurally equivalent (equidistant). (a) Six Fe-Fe J_1 . (b) Six Sm-Sm J_1 . (c) Eight Sm-Fe J_1 . (d) Schematic second-neighbors coordination including twelve J_2 -interactions for either Sm-Sm and Fe-Fe pairs; numbers refer to numbering of atoms in (e). The latter shows Sm and Fe sub-structures in the orthorhombic unit cell as a reference.

HSE (meV)	U(6;4.5) eV	U(5;4.5) eV	U(7;4.5) eV	U(6;4) eV
J_1 (Fe-Fe)	$\simeq 5.85$	$\simeq 5.82$	$\simeq 5.86$	$\simeq 6.25$
J_1 (Sm-Sm)	$\simeq 0.00$	$\simeq -0.01$	$\simeq 0.00$	$\simeq 0.00$
J_2 (Fe-Fe)	$\simeq 0.19$	$\simeq 0.19$	$\simeq 0.20$	$\simeq 0.22$
J_2 (Sm-Sm)	$\simeq 0.01$	$\simeq 0.01$	$\simeq 0.01$	$\simeq 0.01$
J_1 (Sm-Fe)	$\simeq 0.01$	$\simeq 0.04$	$\simeq -0.01$	$\simeq 0.01$

Table SIII. Heisenberg spin exchange (HSE) for first (J_1) and second (J_2) Fe-Fe and Sm-Sm neighbor interactions and Sm-Fe first-neighbor interaction estimated with different Hubbard- U corrections [$U(\text{Sm};\text{Fe})$ eV], considering **FM-FM**, **A-A**, **FM-C**, **FM-G**, **C-G** and **G-G** Sm- and Fe- spins configurations among those listed in Table SII. Underlying crystal structure is fixed to the one obtained relaxing within the **G-G** spin order and U -correction of (6;4.5) eV on Sm- f and Fe- d states, respectively.

Symmetry	w/o Sm- f structure						w/ Sm- f structure					
	Sm- f core			Sm- f valence			Sm- f core			Sm- f valence		
	w/o SOC	\mathbf{G}	\mathbf{G}_x	w/ SOC	$\mathbf{G}-\mathbf{G}$	\mathbf{G}_z	w/o SOC	\mathbf{G}	$\mathbf{G}-\mathbf{G}$	FM-G	C-G	$\text{FM}_x \mathbf{C}_y - \text{FM}_x \mathbf{C}_y \mathbf{G}_z$
A_g (1)	110	107	110		112		104	107	107	107	107	107
B_{1g} (1)	110	110	110		114		106	110	110	110	110	108
B_{2g} (1)	134	134	134		131		127	125	125	125	125	128
A_g (2)	139	138	139		145		127	134	134	135	135	134
B_{3g} (1)	150	153	154		150		152	151	151	150	150	152
B_{1g} (2)	160	160	160		162		149	152	152	152	152	152
B_{3g} (2)	236	234	235		244		210	218	218	218	218	215
A_g (3)	247	245	246		245		232	229	229	229	229	224
B_{1g} (3)	281	281	281		277		255	252	253	252	253	253
B_{2g} (2)	313	313	313		314		306	306	306	306	306	304
A_g (4)	319	320	320		322		306	310	310	310	310	309
B_{1g} (4)	345	345	345		345		344	342	342	343	343	341
B_{3g} (3)	354	355	354		353		356	353	354	353	353	352
A_g (5)	386	386	386		389		374	377	376	377	377	375
A_g (6)	417	417	416		415		420	419	419	419	419	418
B_{3g} (4)	426	427	426		424		427	426	426	425	425	425
B_{2g} (3)	425	428	427		421		433	429	428	428	428	429
B_{2g} (4)	449	448	448		445		446	443	443	444	443	443
B_{1g} (5)	460	460	461		460		446	446	446	446	446	445
A_g (7)	468	468	468		466		459	457	457	457	457	457
B_{1g} (6)	512	513	513		516		503	505	505	505	505	505
B_{3g} (5)	597	597	598		593		604	600	600	600	600	600
B_{1g} (7)	619	618	618		616		620	617	617	617	617	617
B_{2g} (5)	648	646	646		645		652	650	650	650	650	650

Table SIV. Phonon frequencies (in cm^{-1}) of the Raman active modes in the *Pbnm* crystal structure excluding (w/o) and including (w/) either Sm- f electrons and SOC contributions. Main AFM **G**-type spin order is considered for Fe-substructure (\mathbf{G}_x and \mathbf{G}_z indicate **G**-type spin order along x and z spatial directions, respectively). **G**-, **FM**-, **C**-type collinear spin orders are considered for the Sm-substructure. The non-collinear $\text{FM}_x \mathbf{C}_y - \text{FM}_x \mathbf{C}_y \mathbf{G}_z$ Sm-Fe spin configuration is also considered. Underlying atomic structure is fixed: to the one optimized excluding both Sm- f electrons and SOC contributions (w/o Sm- f structure), considering collinear **G**-type Fe-spins order and Hubbard- U correction of 4.5 eV on Fe- d states; to the one optimized including Sm- f electrons contribution (w/ Sm- f structure), collinear **G**-type spin order for both Sm and Fe substructures and U of 6 eV and 4.5 eV on the Sm- f and Fe- d states.

Symmetry	w/o Sm- <i>f</i> structure		w/ Sm- <i>f</i> structure		1 GPa structure
Silent and IR modes	Sm- <i>f</i> core	Sm- <i>f</i> valence	Sm- <i>f</i> core	Sm- <i>f</i> valence	Sm- <i>f</i> valence
A _u (1)	86	74	86	79	79
B _{2u} (1)	104	102	100	103	104
B _{3u} (1)	113	114	102	106	107
B _{1u} (1)	159	156	148	140	144
A _u (2)	161	152	152	156	156
B _{3u} (2)	175	182	161	172	174
B _{1u} (2)	171	182	156	181	180
B _{2u} (2)	191	189	181	184	185
A _u (3)	208	184	188	187	183
B _{2u} (3)	245	241	226	233	233
A _u (4)	248	246	235	236	238
B _{1u} (3)	273		262	243	266
B _{3u} (3)	256	249/274	245	249	250
B _{3u} (4)	281	317	271	271	272
B _{2u} (4)	289	288	276	279	280
A _u (5)	300	294	293	290	291
B _{2u} (5)	308	302	299	300	302
B _{3u} (5)	320	317	308	309	309
B _{2u} (6)	331	328	320	321	323
B _{1u} (4)	302	333	296	330	339
B _{3u} (6)	349	339	341	338	340
A _u (6)	354	349	351	347	350
B _{3u} (7)	386	379	376	371	374
B _{1u} (5)	354	386	347	378	350
B _{2u} (7)	417	417	409	409	412
B _{3u} (8)	474	477	459	461	464
B _{2u} (8)	512	510	507	506	509
A _u (7)	504	499	511	506	513
B _{1u} (6)	501	509	502	513	505
B _{2u} (9)	524	521	522	520	525
A _u (8)	523	519	530	526	532
B _{3u} (9)	545	543	547	540	550
B _{1u} (7)	536	536	545	544	546

Table SV. Phonon frequencies (in cm⁻¹) of the silent and infrared (IR) active modes in the *Pbnm* crystal structure, considering collinear G-type AFM magnetic ordering for Fe atoms when freezing Sm-*f* electrons in the core states, and for both Sm and Fe sub-structures when including those in VB.